
Correlation Priors for Reinforcement Learning

Bastian Alt*, Adrian Šošić* and Heinz Koepl

Department of Electrical Engineering and Information Technology
Technische Universität Darmstadt

{bastian.alt, adrian.sosic, heinz.koepl}@bcs.tu-darmstadt.de

Abstract

Many decision-making problems naturally exhibit pronounced structures inherited from the underlying characteristics of the environment. In a Markov decision process model, for example, two distinct states can have inherently related semantics or encode resembling physical state configurations, often implying locally correlated transition dynamics among the states. In order to complete a certain task, an agent acting in such environments needs to execute a series of temporally and spatially correlated actions. Though there exists a variety of approaches to account for correlations in continuous state-action domains, a principled solution for discrete environments is missing. In this work, we present a Bayesian learning framework based on Pólya-Gamma augmentation that enables an analogous reasoning in such cases. We demonstrate the framework on a number of common decision-making related tasks, such as reinforcement learning, imitation learning and system identification. By explicitly modeling the underlying correlation structures, the proposed approach yields superior predictive performance compared to correlation-agnostic models, even when trained on data sets that are up to an order of magnitude smaller in size.

1 Introduction

Correlations arise naturally in many aspects of decision-making. The reason for this phenomenon is that decision-making problems usually exhibit pronounced *structures*, which substantially influence the strategies of an agent. Examples of such correlations can even occur in stateless decision-making problems, such as multi-armed bandits, where prominent patterns in the reward mechanisms of different arms will translate to correlations between the action choices of the agent [7, 8]. These statistical relationships are especially pronounced in the case of contextual bandits, where effective decision-strategies not only exhibit temporal correlation but also take into account the state context at each time point, introducing a second source of correlation [10]. In more general decision-making models, such as Markov decision processes (MDPs), the agent can directly affect the state of the environment through its action choices. In many cases, the effects caused by these actions share common patterns between different states of the process, often because the states have inherently related semantics or encode similar physical state configurations of the underlying system. Examples of this general principle are omnipresent in all disciplines and range from robotics, where similar actuator outputs result in similar kinematic responses for similar states of the robot’s joints, to networking applications, where the servicing of a particular queue affects primarily the local network state (Section 4). The common consequence is that the structures of the environment are reflected in the decision of the operating agent, who needs to execute a series of temporally and spatially dependent actions in order to complete a certain task. This is particularly true when two or more agents interact with each other in the same environment and need coordinate their behavior [2].

When focusing on rational behavior, correlations manifest themselves even in unstructured domains, though at a higher level of abstraction of the decision-making process. This is because rationality itself

* The first two authors contributed equally to this work.

implies the existence of an underlying objective optimized by the agent that represents the agent’s intentions and incentivizes to choose one action over another. These goals are typically constant at least for a certain periods of time, which inevitably causes dependencies between consecutive action choices.

In this paper, we introduce a learning framework that offers a direct way to model such correlations in *finite* decision-making problems, i.e., systems with discrete state and action spaces. A key feature of the framework is that it allows to capture correlations at any level of the process, that is, at the level of the system environment, at the intentional level, or directly at the level of the executed actions. We encode the underlying structure in a hierarchical Bayesian model, for which we derive a tractable variational inference method based on Pólya-Gamma augmentation that allows a fully probabilistic treatment of the learning problem. Results on common benchmark problems and a queuing network simulation demonstrate the advantages of the framework.

Related Work

Modeling correlations in decision-making is a common theme in reinforcement learning and related fields. Gaussian processes (GPs) offer a flexible tool for this purpose and are widely used in a broad variety of contexts. Moreover, movement primitives [15] provide an effective way to describe temporal relationships in control problems. However, the natural problem domain of both are continuous state-action environments, which lie outside the scope of this work.

Inferring correlation structure from count data has been discussed extensively in the context of topic modeling [11, 12] and factor analysis [22]. Recently, [23] proposed a GP classification algorithm with a scalable variational approach based on Pólya-Gamma augmentation. Though these approaches are promising, they do not discuss the problem of decision-making.

For agents acting in discrete environments, a number of customized solutions exist that allow to model specific aspects of the problem. A broad class of methods that specifically target temporal correlations are based on hidden Markov models. Many of these approaches operate on the intentional level, modeling the temporal relationships of the different goals followed by the agent [17]. However, there also exist approaches to capture spatial dependencies between the goals. For a recent overview, see [20] and the references therein. Dependencies on the action level have been also considered in the past though existing approaches mostly focus on the temporal correlations between actions, such as probabilistic movement primitives [15], or are restricted to deterministic policy models. A probabilistic framework to capture correlations between discrete action distributions is described in [19]. When it comes to modeling transition dynamics, most existing approaches rely on GP models [4, 3]. To the best of our knowledge, there exists no principled method that explicitly models correlations in the transition dynamics of discrete environments. A universally applicable framework for discrete environments that is comparable to Gaussian processes has not yet emerged. The goal of this paper is to fill this gap by providing a flexible inference framework for such cases.

2 Background

2.1 Markov Decision Processes

In this paper, we consider finite Markov decision processes (MDPs) of the form $(\mathcal{S}, \mathcal{A}, \mathcal{T}, R)$, where $\mathcal{S} = \{1, \dots, S\}$ is a finite state space containing S distinct states, $\mathcal{A} = \{1, \dots, A\}$ is an action space comprising A actions for each state, $\mathcal{T} : \mathcal{S} \times \mathcal{S} \times \mathcal{A} \rightarrow [0, 1]$ is the state transition model specifying the probability distribution over next states for each current state and action, and $R : \mathcal{S} \times \mathcal{A} \rightarrow \mathbb{R}$ is a reward function. For further details, see [21].

2.2 Inference in MDPs

In decision-making with discrete state and action spaces, we are often faced with integer-valued quantities modeled as draws from multinomial distributions $\mathbf{x}_c \sim \text{Mult}(\mathbf{x}_c \mid N_c, \mathbf{p}_c)$, where $c \in \mathcal{C}$ indexes some finite covariate space with cardinality C and $\mathbf{p}_c \in \Delta^K$, $N_c \in \mathbb{N}$ parametrizes the distribution at the given covariate value c . Herein, \mathbf{x}_c can either represent actual count data observed during an experiment or describe some latent variable of our model. For example, when modeling the policy of an agent in an MDP, \mathbf{x}_c may represent the vector of action counts observed at a given state

s , in which case $\mathcal{C} = \mathcal{S}$, $K = A$, and N_c is the total number of times we observe the agent choosing an action at state c . Similarly, when modeling state transition probabilities, \mathbf{x}_c could be the vector counting outgoing transitions from some state s for a given action a (in which case $\mathcal{C} = \mathcal{S} \times A$) or, in the context of modeling the agent’s intentions, \mathbf{x}_c could describe the number of times the agent follows a particular goal, which itself might be unobservable [20].

When solving the inverse problem of inferring the probability vectors $\{\mathbf{p}_c\}$ from the count data $\{\mathbf{x}_c\}$, a computationally straightforward approach is to model the probability vectors as independent Dirichlet distributions for all covariate values, i.e., $\mathbf{p}_c \sim \text{Dir}(\mathbf{p}_c \mid \boldsymbol{\alpha}_c) \forall c \in \mathcal{C}$, where $\boldsymbol{\alpha}_c$ describes a local concentration parameter. However, the resulting model is agnostic to the rich correlation structure present in most MDPs (Section 1) and thus ignores much of the prior information we have about the underlying decision-making problem. A more natural approach would be to model the probability vectors $\{\mathbf{p}_c\}$ jointly using common prior, in order to capture their dependency structure. Unfortunately, this renders exact posterior inference intractable, since the resulting prior models are no longer conjugate to the multinomial likelihood.

Recently, a method for approximate inference in dependent multinomial models has been developed in [12] to account for the inherent correlation of the probability vectors. To this end, the following prior model was introduced,

$$\mathbf{p}_c = \Pi_{\text{SB}}(\boldsymbol{\psi}_{c \cdot}), \quad \boldsymbol{\psi}_{\cdot k} \sim \mathcal{N}(\boldsymbol{\psi}_{\cdot k} \mid \boldsymbol{\mu}_k, \boldsymbol{\Sigma}), \quad k = 1, \dots, K-1. \quad (1)$$

Herein, $\Pi_{\text{SB}}(\boldsymbol{\zeta}) = [\Pi_{\text{SB}}^{(1)}(\boldsymbol{\zeta}), \dots, \Pi_{\text{SB}}^{(K)}(\boldsymbol{\zeta})]^\top$ is the *logistic stick-breaking transformation*, where

$$\Pi_{\text{SB}}^{(k)}(\boldsymbol{\zeta}) = \sigma(\zeta_k) \prod_{j < k} (1 - \sigma(\zeta_j)), \quad k = 1, \dots, K-1, \quad \Pi_{\text{SB}}^{(K)}(\boldsymbol{\zeta}) = 1 - \sum_{k=1}^{K-1} \Pi_{\text{SB}}^{(k)}(\boldsymbol{\zeta}),$$

and σ is the logistic function. The purpose of this transformation is to map the real-valued Gaussian variables to the simplex by passing each entry through the sigmoid function and subsequently following a regular stick-breaking construction [9]. Through the correlation structure $\boldsymbol{\Sigma}$ of the latent variables $\boldsymbol{\Psi}$, the transformed probability vectors $\{\mathbf{p}_c\}$ become dependent. Posterior inference for the latent variables $\boldsymbol{\Psi}$ can be traced out efficiently by introducing a set of auxiliary Pólya-Gamma (PG) variables, which leads to a conjugate model in the augmented space. This enables a simple inference procedure based on blocked Gibbs sampling, where the Gaussian variables and PG variables are sampled in turn conditioned on each other and the count data $\{\mathbf{x}_c\}$.

In the following section, we present a variational inference (VI) [1] approach utilizing this augmentation trick, which establishes a closed-form approximation for the posterior distribution. Moreover, we present a hyper-parameter optimization method based on variational expectation-maximization that allows us to calibrate our model to a particular problem type, avoiding the need for manual parameter tuning. This enables us to go beyond existing sampling-based approaches, providing a fast inference algorithm for correlated count data.

3 Variational Inference for Dependent Multinomial Models

The goal of our inference procedure is to calculate the posterior distribution $p(\boldsymbol{\Psi} \mid \mathbf{X})$, where $\mathbf{X} = [\mathbf{x}_1, \dots, \mathbf{x}_C]$ is the data matrix and $\boldsymbol{\Psi} = [\boldsymbol{\psi}_{\cdot 1}, \dots, \boldsymbol{\psi}_{\cdot K-1}]$ is the matrix of real-valued parameters. Exact inference is intractable since the calculation of $p(\boldsymbol{\Psi} \mid \mathbf{X})$ requires marginalization over the joint parameter space of all variables $\boldsymbol{\Psi}$. Instead of following a Monte Carlo approach as in [12], we resort to a variational approximation. To this end, we search for the best approximating distribution from a family of distributions $\mathcal{Q}_{\boldsymbol{\Psi}}$ such that

$$p(\boldsymbol{\Psi} \mid \mathbf{X}) \approx q^*(\boldsymbol{\Psi}) = \arg \min_{q(\boldsymbol{\Psi}) \in \mathcal{Q}_{\boldsymbol{\Psi}}} \text{KL}(q(\boldsymbol{\Psi}) \parallel p(\boldsymbol{\Psi} \mid \mathbf{X})). \quad (2)$$

Carrying out this optimization under a multinomial likelihood is hard because it involves intractable expectations over the variational distribution. However, in the following we show that, analogously to the inference scheme of [12], a Pólya-Gamma data augmentation of $\boldsymbol{\Psi}$ makes the optimization tractable. To this end, we introduce a family of augmented posterior distributions $\mathcal{Q}_{\boldsymbol{\Psi}, \boldsymbol{\Omega}}$ and consider the problem

$$p(\boldsymbol{\Psi}, \boldsymbol{\Omega} \mid \mathbf{X}) \approx q^*(\boldsymbol{\Psi}, \boldsymbol{\Omega}) = \arg \min_{q(\boldsymbol{\Psi}, \boldsymbol{\Omega}) \in \mathcal{Q}_{\boldsymbol{\Psi}, \boldsymbol{\Omega}}} \text{KL}(q(\boldsymbol{\Psi}, \boldsymbol{\Omega}) \parallel p(\boldsymbol{\Psi}, \boldsymbol{\Omega} \mid \mathbf{X})), \quad (3)$$

where $\mathbf{\Omega} = [\omega_1, \dots, \omega_{K-1}] \subseteq \mathbb{R}^{C \times K-1}$ denotes the matrix of auxiliary variables. Notice that the desired posterior can be recovered as the marginal $p(\mathbf{\Psi} | \mathbf{X}) = \int p(\mathbf{\Psi}, \mathbf{\Omega} | \mathbf{X}) d\mathbf{\Omega}$.

First, we note that solving the optimization problem is equivalent to maximizing the evidence lower bound (ELBO)

$$\log p(\mathbf{X}) \geq L(q) = \mathbb{E} [\log p(\mathbf{\Psi}, \mathbf{\Omega}, \mathbf{X})] - \mathbb{E} [\log q(\mathbf{\Psi}, \mathbf{\Omega})],$$

where the expectations are calculated w.r.t. the variational distribution $q(\mathbf{\Psi}, \mathbf{\Omega})$. In order to arrive at a tractable expression for the ELBO, we recapitulate the following data augmentation scheme derived in [12],

$$\begin{aligned} p(\mathbf{\Psi}, \mathbf{X}) &= \left(\prod_{k=1}^{K-1} \mathcal{N}(\psi_{\cdot k} | \mu_k, \Sigma) \right) \left(\prod_{c=1}^C \text{Mult}(\mathbf{x}_c | N_c, \mathbf{\Pi}_{\text{SB}}(\psi_c)) \right) \\ &= \left(\prod_{k=1}^{K-1} \mathcal{N}(\psi_{\cdot k} | \mu_k, \Sigma) \right) \left(\prod_{c=1}^C \prod_{k=1}^{K-1} \text{Bin}(x_{ck} | b_{ck}, \sigma(\psi_{ck})) \right). \end{aligned}$$

The stick-breaking representation of the multinomial distribution is expanded using $b_{ck} = N_c - \sum_{j < k} x_{cj}$. Furthermore, we have

$$p(\mathbf{\Psi}, \mathbf{X}) = \left(\prod_{k=1}^{K-1} \mathcal{N}(\psi_{\cdot k} | \mu_k, \Sigma) \right) \left(\prod_{c=1}^C \prod_{k=1}^{K-1} \binom{b_{ck}}{x_{ck}} \sigma(\psi_{ck})^{x_{ck}} (1 - \sigma(\psi_{ck}))^{b_{ck} - x_{ck}} \right)$$

and finally, the Pólya-Gamma variable augmentation introduced in [16] is obtained using the integral identity

$$= \underbrace{\int \prod_{k=1}^{K-1} \mathcal{N}(\psi_{\cdot k} | \mu_k, \Sigma) \prod_{c=1}^C \binom{b_{ck}}{x_{ck}} 2^{-b_{ck}} \exp(\kappa_{ck} \psi_{ck}) \exp(-\omega_{ck} \psi_{ck}^2 / 2) \text{PG}(\omega_{ck} | b_{ck}, 0) d\mathbf{\Omega}}_{p(\mathbf{\Psi}, \mathbf{\Omega}, \mathbf{X})}.$$

Herein, $\kappa_{ck} = x_{ck} - b_{ck}/2$ and $\text{PG}(\zeta | u, v)$ is the density of the Pólya-Gamma distribution, with the exponential tilting property $\text{PG}(\zeta | u, v) = \frac{\exp(-\frac{v^2}{2}\zeta) \text{PG}(\zeta | u, 0)}{\cosh^{-u}(v/2)}$ and the first moment $\mathbb{E}[\zeta] = \frac{u}{2v} \tanh(v/2)$. With this augmented distribution at hand, we derive a mean-field approximation for the variational distribution as

$$q(\mathbf{\Psi}, \mathbf{\Omega}) = \prod_{k=1}^{K-1} q(\psi_{\cdot k}) \prod_{c=1}^C q(\omega_{ck}).$$

Exploiting calculus of variations, we obtain the following parametric forms for the components of the variational distributions,

$$q(\psi_{\cdot k}) = \mathcal{N}(\psi_{\cdot k} | \lambda_k, \mathbf{V}_k), \quad q(\omega_{ck}) = \text{PG}(\omega_{ck} | b_{ck}, w_{ck}).$$

The optimal parameters and first moments of the variational distributions are

$$w_{ck} = \sqrt{\mathbb{E}[\psi_{ck}^2]}, \quad \mathbf{V}_k = (\mathbf{\Sigma}^{-1} + \text{diag}(\mathbb{E}[\omega_k]))^{-1}, \quad \lambda_k = \mathbf{V}_k(\kappa_k + \mathbf{\Sigma}^{-1} \mu_k),$$

$$\mathbb{E}[\psi_{ck}^2] = ((\mathbf{V}_k)_{cc} + \lambda_{ck}^2), \quad \mathbb{E}[\omega_{ck}] = \frac{b_{ck}}{2w_{ck}} \tanh(w_{ck}/2),$$

with $\omega_k = [\omega_{1k}, \dots, \omega_{Ck}]^\top$ and $\kappa_k = [\kappa_{1k}, \dots, \kappa_{Ck}]^\top$. A detailed derivation of these results and the resulting ELBO is provided in Appendix A. The variational approximation can be optimized using coordinate-wise ascent by cycling through the parameters and their moments. The corresponding distribution over probability vectors $\{\mathbf{p}_c\}$ is defined implicitly through the deterministic relationship in Eq. (1).

3.1 Hyper-Parameter Optimization

For hyper-parameter learning, we employ a variational expectation-maximization approach [13] to optimize the ELBO after each update of the variational parameters. Assuming a covariance matrix Σ_θ parametrized by a set of parameters $\theta = [\theta_1, \dots, \theta_J]^\top$, the ELBO can be written as

$$\begin{aligned} L(q) = & -\frac{K-1}{2} |\Sigma_\theta| + \frac{1}{2} \sum_{k=1}^{K-1} \log |\mathbf{V}_k| - \frac{1}{2} \sum_{k=1}^{K-1} \text{tr}(\Sigma_\theta^{-1} \mathbf{V}_k) \\ & - \frac{1}{2} \sum_{k=1}^{K-1} (\mu_k - \lambda_k)^\top \Sigma_\theta^{-1} (\mu_k - \lambda_k) + C(K-1) + \sum_{k=1}^{K-1} \sum_{c=1}^C \log \left(\frac{b_{ck}}{x_{ck}} \right) \\ & - \sum_{k=1}^{K-1} \sum_{c=1}^C b_{ck} \log 2 + \sum_{k=1}^{K-1} \lambda_k^\top \kappa_k - \sum_{k=1}^{K-1} \sum_{c=1}^C b_{ck} \log \left(\cosh \frac{w_{ck}}{2} \right). \end{aligned}$$

A detailed derivation can be found in Appendix A.2. The corresponding gradients w.r.t. the hyper-parameters calculate to

$$\begin{aligned} \frac{\partial L}{\partial \mu_k} = \Sigma_\theta^{-1} (\mu_k - \lambda_k), \quad \frac{\partial L}{\partial \theta_j} = & -\frac{1}{2} \sum_{k=1}^{K-1} \left(\text{tr}(\Sigma_\theta^{-1} \frac{\partial \Sigma_\theta}{\partial \theta_j}) - \text{tr}(\Sigma_\theta^{-1} \frac{\partial \Sigma_\theta}{\partial \theta_j} \Sigma_\theta^{-1} \mathbf{V}_k) \right. \\ & \left. - (\mu_k - \lambda_k)^\top \Sigma_\theta^{-1} \frac{\partial \Sigma_\theta}{\partial \theta_j} \Sigma_\theta^{-1} (\mu_k - \lambda_k) \right), \end{aligned}$$

which admits a closed-form solution for the optimal mean parameters, given by $\mu_k = \lambda_k$.

For the optimization of the covariance parameters, one could resort to a numerical scheme; however, this requires a full inversion of the covariance matrix in each update. As it turns out, a closed-form expression can be found for the special case when θ is a scale parameter, i.e., $\Sigma_\theta = \theta \tilde{\Sigma}$, for some fixed $\tilde{\Sigma}$. The optimal parameter value can then be determined as

$$\theta = \frac{1}{KC} \sum_{k=1}^{K-1} \text{tr} \left(\tilde{\Sigma}^{-1} (\mathbf{V}_k + (\mu_k - \lambda_k)(\mu_k - \lambda_k)^\top) \right).$$

The closed-form solution avoids repeated matrix inversions since $\tilde{\Sigma}^{-1}$, being independent of all hyper-parameters and variational parameters, can be evaluated at the start of the algorithm. The full derivation of the gradients and the closed-form expressions is provided in Appendix B.

For the experiments in the following section, we restrict ourselves to a squared exponential covariance function $(\Sigma_\theta)_{cc'} = \theta \exp \left(-\frac{d(c, c')^2}{l^2} \right)$, with a covariate distance measure $d : \mathcal{C} \times \mathcal{C} \rightarrow \mathbb{R}_{\geq 0}$ and length scale $l \in \mathbb{R}_{\geq 0}$ adapted to the specific modeling scenario. Yet, we note that multiple covariance functions can be easily compared against each other for model selection based on the resulting values of the ELBO [13]. Also, a combination of functions can be employed, as long as the resulting covariance matrix is positive semi-definite (see covariance kernels of GPs [18]).

4 Experiments

To demonstrate the versatility of our inference framework, we test it on a number of different modeling scenarios that commonly occur in decision-making contexts. Due to space limitations, we restrict ourselves to imitation learning, system identification, and Bayesian reinforcement learning. However, we would like to point out that the same modeling principles can be applied to many other scenarios, such as subgoal extraction [20] or behavior coordination among agents [2], to name only two examples. A more comprehensive evaluation study is left for future work.

4.1 Imitation Learning

First, we illustrate our framework on an imitation learning example, where we aspire to reconstruct the policy of an agent (in this context called the *expert*) from observed behavior. For the reconstruction,

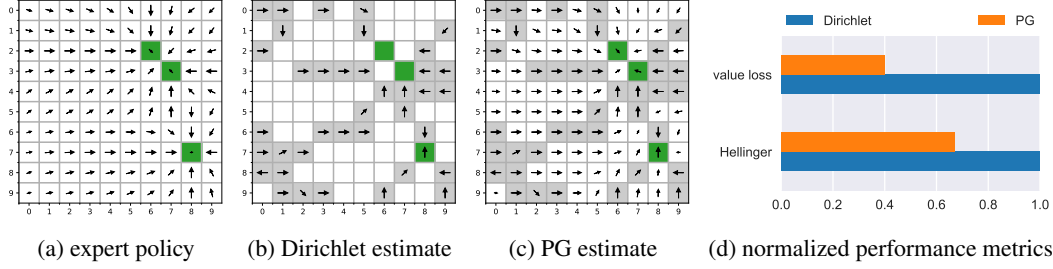


Figure 1: Imitation learning example. The expert policy in (a) is reconstructed using the posterior mean estimates of (b) an independent Dirichlet policy model and (c) a correlated PG model, based on action data observed at the states marked in gray. The joint estimation of the local policies yields a significantly improved reconstruction, as shown by the resulting Hellinger distance to the expert policy and the corresponding value loss [20] in (d).

we suppose to have access to a demonstration data set $\mathcal{D} = \{(s_d, a_d) \in \mathcal{S} \times \mathcal{A}\}_{d=1}^D$ containing D state-action pairs, where each action has been generated according to the expert’s policy, i.e., $a_d \sim \pi(a | s_d)$. Assuming a discrete state and action space, the policy of the agent can be represented as a stochastic matrix $\mathbf{\Pi} = [\pi_1, \dots, \pi_S]$, whose i th column $\pi_i \in \Delta^A$ represents the local distribution over actions selected by the agent at state i . Our goal is to estimate this matrix from the demonstrations \mathcal{D} . By constructing the count matrix $(\mathbf{X})_{ij} = \sum_{d=1}^D \mathbb{1}(s_d = i \wedge a_d = j)$, the inference problem can be directly mapped to our PG model, which allows to jointly estimate the coupled quantities $\{\pi_i\}$ through their latent representation Ψ by approximating the posterior distribution $p(\Psi | \mathbf{X})$ in Eq. (2). In this case, the covariate set \mathcal{C} is described by the state space \mathcal{S} .

To demonstrate the advantages of this joint inference approach over a correlation-agnostic estimation method, we compare our framework to the independent Dirichlet model described in Section 2.2. Both reconstruction methods are evaluated on a classical grid world scenario comprising $S = 100$ states and $A = 4$ actions. Each action triggers a noisy transition in one of the four cardinal directions such that pattern of the resulting next-state distribution resembles a discretized Gaussian distribution centered around the targeted adjacent state. Rewards are distributed randomly in the environment. The expert follows a near-optimal stochastic policy, choosing actions from a softmax distribution resulting from the Q-values at the current state. An example scenario is shown in Fig. 1a, where the displayed arrows are obtained by weighting the four unit vectors associated with the action set \mathcal{A} according to their local action probabilities. The reward locations are highlighted in green.

Fig. 1b shows the reconstruction of the policy obtained through the independent Dirichlet model. Since, no dependencies between the states are considered in this approach, a posterior estimate can only be obtained for states at which demonstration data is available, highlighted by the gray coloring of the background. For all remaining states, the mean estimate predicts a uniform action choice for the expert behavior since no action is preferred by the symmetry of the prior, resulting in an effective arrow length of zero. By contrast, the PG model (Fig. 1c) is able to generalize the expert behavior to unobserved regions of the state space, resulting in significantly improved reconstruction of the policy (Fig. 1d). To capture the underlying correlations, we used the Euclidean distance between the grid positions as distance measure d and set l to the maximal occurring distance value.

4.2 System Identification & Bayesian Reinforcement Learning

Having focused all attention on learning a model of a given policy, we now enter the realm of Bayesian reinforcement learning (BRL) and try to optimize our behavior to the particular dynamics of an environment. For this purpose, we modify our grid world from Section 4.1 slightly by placing a target reward of +1 in one corner and transporting the agent back to the opposite corner when reaching the target (see “Grid10” domain in [6]). For the experiment, we assume that the agent is aware of the target reward but does not know the transition dynamics of the environment.

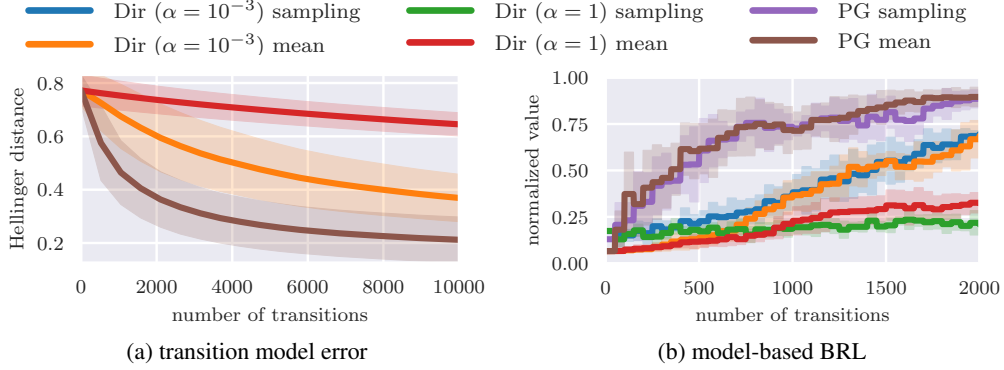


Figure 2: Bayesian reinforcement learning results. (a) Estimation error of the transition dynamics over the number of observed transitions. Shown are the Hellinger distances to the true next-state distribution and the standard deviation of the estimation error, both averaged over all states and action of the MDP. (b) Expected returns (normalized by the optimal return) of the policies obtained when re-planning with the estimated transition dynamics after every fiftieth state transition.

4.2.1 System Identification

For the beginning, we ignore the reward mechanism altogether and focus on learning the transition dynamics of the environment. To this end, we let the agent perform a random walk on the grid, choosing actions uniformly at random and observing the resulting state transitions. The recorded state-action sequence $(s_1, a_1, s_2, a_2, \dots, a_{T-1}, s_T)$ is summarized in the form of count matrices $[\mathbf{X}^{(1)}, \dots, \mathbf{X}^{(A)}]$, where the element $(\mathbf{X}^{(a)})_{ij} = \sum_{t=1}^T \mathbb{1}(a_t = a \wedge s_t = i \wedge s_{t+1} = j)$ represents the number of observed transitions from state i to j for action a . Analogously to the imitation learning experiment in Section 4.1, we estimate the transition dynamics of the environment from these matrices using an independent Dirichlet prior model and our PG framework, where we employ a separate model for each transition count matrix. The resulting estimation accuracy is described by the graphs in Fig. 2a, which show the distance between the ground truth dynamics of the environment and those predicted by the models, averaged over all states and actions. As before, our PG model significantly outperforms the naive Dirichlet approach.

4.2.2 Bayesian Reinforcement Learning

Next, we consider the problem of combined model-learning and decision-making by utilizing the experience from earlier interactions to optimize our future behavior. Bayesian reinforcement learning offers a natural and flexible playground for this task as it intrinsically balances the importance of information gathering and instantaneous reward maximization, avoiding the exploration-exploitation dilemma encountered in classical reinforcement learning schemes [5].

To find the optimal trade-off between the these two competing objectives, we follow the principle of *posterior sampling for reinforcement learning* (PSRL) [14], where future actions are planned using a probabilistic model of the environment’s transition dynamics. Herein, we consider two variants: (i) in the first variant, we compute the optimal state-action values for a fixed number of posterior samples of the transition dynamics and select the actions that yield the highest expected return on average. (ii) In the second variant, we take the greedy action dictated by the posterior mean of the transition dynamics. In both cases, the obtained policy is followed for a fixed number of transitions before new observations are taken into account in the posterior distribution. Fig. 2b shows the expected returns of the so-obtained strategies over the entire execution period for the three prior models evaluated in Fig. 2a and both PSRL variants. The graphs reveal that the PG approach requires significantly fewer transitions to learn an effective decision-making strategy.

4.2.3 Queuing Network Modeling

Finally, we evaluate our model on a two-server queuing network, as depicted in Fig. 3a. The network consists of two queues with buffer lengths $B_1 = B_2 = 10$. The state of the system is determined by

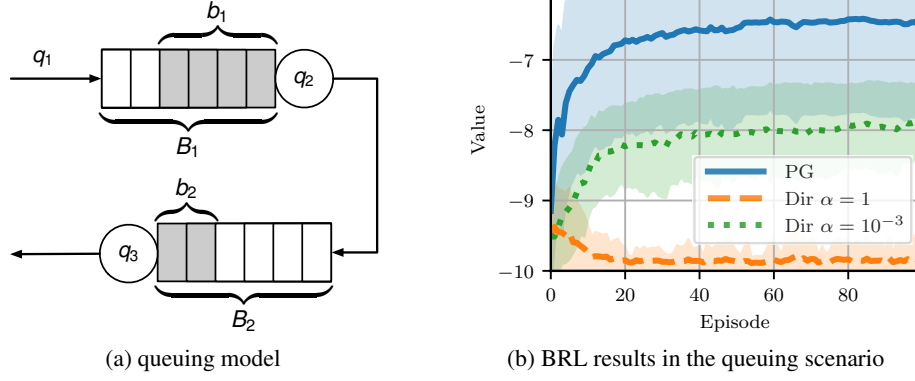


Figure 3: BRL in batch queuing. (a) The batch queuing model has a discrete input stream q_1 . The agent processes the packets either from the first or the second queue, where the packets are processed as batches using the server capacity q_2 or q_3 . The state of the system are the queue fillings b_1 and b_2 in a finite buffer regime. (b) Average value of policies per episode of twenty state transitions.

the number of packets in each queue, summarized by the queuing vector $\mathbf{b} = [b_1, b_2]^\top$, where b_1 and b_2 are the number of packets in queue 1 and 2, respectively. Hence, $\mathcal{S} = \{0, \dots, B_1\} \times \{0, \dots, B_2\}$ and the size of the state space is $S = (B_1 + 1)(B_2 + 1)$. For our experiment, we consider a system with batch arrivals and batch servicing. The task for the agent is to schedule the traffic flow of the network, considering that only one of the queues can be processed at a time. The actions are encoded as $a = 1$ for serving queue 1 and $a = 2$ for serving queue 2. The number of packets arriving at queue 1 is modeled as $q_1 \sim \text{Pois}(q_1 | \vartheta_1)$ with mean rate $\vartheta_1 = 1$. The packages are transferred to buffer 1 and subsequently processed in batches of a random size $q_2 \sim \text{Pois}(q_2 | \vartheta_2)$, provided that the agent selects queue 1. Therefore, $\vartheta_2 = \beta_1 \mathbb{1}(a = 1)$, where we consider an average batch size of $\beta_1 = 3$. The processed packets are transferred to the second queue, where they wait to be processed by the agent in batches of size, $q_3 \sim \text{Pois}(q_3 | \vartheta_3)$, with $\vartheta_3 = \beta_2 \mathbb{1}(a = 2)$ and an average batch size of $\beta_2 = 2$. The resulting transition dynamics can be compactly written as

$$\begin{bmatrix} b'_1 \\ b'_2 \end{bmatrix} = \begin{bmatrix} (b_1 + q_1 - q_2)_0^{B_1} \\ (b_2 + q_2 - q_3)_0^{B_2} \end{bmatrix} \quad (4)$$

where the truncation operation $(\cdot)_0^B = \max(0, \min(B, \cdot))$ accounts for the nonnegativity and finiteness of the buffers and $\mathbf{b}' = [b'_1, b'_2]^\top$ describes the new queuing state after the processing step. The reward function, which is known to the agent, computes the negative sum of the queue lengths $R(\mathbf{b}) = -(b_1 + b_2)$. Despite the simplistic architecture of the network, finding an optimal policy for this problem is challenging, since determining the state transition matrices requires nontrivial calculations involving concatenation of Poisson distributions. More importantly, when applied in a real-world context, the rates of the system are typically unknown and planning-based methods cannot be applied.

Fig. 3b shows the evaluation of PSRL on the network. As in the previous experiment, we use a separate PG model for action. Again, the covariance is computed based on the normalized Euclidean distance between the queuing states of the system, encoding our prior knowledge that the system states obtained after servicing two independent copies of the system will look more similar if their queuing states before the servicing time were similar. The agent follows a greedy strategy w.r.t. the posterior mean of the estimated model. The policy is evaluated after each policy update by performing one thousand steps from all possible queuing states of the system. Again, the PG approach significantly outperforms the correlation agnostic prior, requiring fewer interactions with the system while yielding better scheduling strategies by generalizing the system dynamics over queuing states.

5 Conclusion

We have presented a self-contained learning framework for flexible use in many common decision-making contexts. The framework allows an intuitive consideration of prior knowledge about the structures of the environment and the behavior of an agent, which significantly increases the predictive

performance of the resulting model by leveraging correlations and reoccurring patterns in the decision-making process. A key feature is the automatic calibration of the model hyper-parameters through adjustment of the model regularization to the specific decision-making scenario at hand, which provides a built-in solution to infer the effective range of the correlations from the data. We have evaluated the framework on various benchmark tasks and on a realistic queuing problem, which in a real-world situation admits no planning-based solution due to unknown system parameters. In all considered scenarios, our framework significantly outperformed the naive baseline methods that neglect the intrinsic statistical relationships of the problems.

Acknowledgments

This work has been funded by the German Research Foundation (DFG) as part of the project B4 within the Collaborative Research Center (CRC) 1053 – MAKI.

References

- [1] D. M. Blei, A. Kucukelbir, and J. D. McAuliffe. Variational inference: A review for statisticians. *Journal of the American Statistical Association*, 112(518):859–877, 2017.
- [2] G. Chalkiadakis and C. Boutilier. Coordination in multiagent reinforcement learning: A Bayesian approach. In *Proceedings of the 2nd International Joint Conference on Autonomous Agents and Multiagent Systems*, pages 709–716. ACM, 2003.
- [3] M. Deisenroth and C. E. Rasmussen. Pilco: A model-based and data-efficient approach to policy search. In *Proceedings of the 28th International Conference on Machine Learning*, pages 465–472, 2011.
- [4] Y. Engel, S. Mannor, and R. Meir. Bayes meets bellman: The Gaussian process approach to temporal difference learning. In *Proceedings of the 20th International Conference on Machine Learning*, pages 154–161, 2003.
- [5] M. Ghavamzadeh, S. Mannor, J. Pineau, A. Tamar, et al. Bayesian reinforcement learning: A survey. *Foundations and Trends in Machine Learning*, 8(5-6):359–483, 2015.
- [6] A. Guez, D. Silver, and P. Dayan. Efficient Bayes-adaptive reinforcement learning using sample-based search. In *Advances in Neural Information Processing Systems*, pages 1025–1033, 2012.
- [7] S. Gupta, G. Joshi, and O. Yağın. Correlated multi-armed bandits with a latent random source. *arXiv preprint arXiv:1808.05904*, 2018.
- [8] M. Hoffman, B. Shahriari, and N. Freitas. On correlation and budget constraints in model-based bandit optimization with application to automatic machine learning. In *Artificial Intelligence and Statistics*, pages 365–374, 2014.
- [9] H. Ishwaran and L. F. James. Gibbs sampling methods for stick-breaking priors. *Journal of the American Statistical Association*, 96(453):161–173, 2001.
- [10] A. Krause and C. S. Ong. Contextual Gaussian process bandit optimization. In *Advances in Neural Information Processing Systems*, pages 2447–2455, 2011.
- [11] J. D. Lafferty and D. M. Blei. Correlated topic models. In *Advances in Neural Information Processing Systems*, pages 147–154, 2006.
- [12] S. Linderman, M. Johnson, and R. P. Adams. Dependent multinomial models made easy: Stick-breaking with the pólya-gamma augmentation. In *Advances in Neural Information Processing Systems*, pages 3456–3464, 2015.
- [13] K. P. Murphy. *Machine learning: a probabilistic perspective*. MIT Press, 2012.
- [14] I. Osband, D. Russo, and B. Van Roy. (More) efficient reinforcement learning via posterior sampling. In *Advances in Neural Information Processing Systems*, pages 3003–3011, 2013.
- [15] A. Paraschos, C. Daniel, J. R. Peters, and G. Neumann. Probabilistic movement primitives. In *Advances in Neural Information Processing Systems*, pages 2616–2624, 2013.
- [16] N. G. Polson, J. G. Scott, and J. Windle. Bayesian inference for logistic models using Pólya-gamma latent variables. *Journal of the American statistical Association*, 108(504):1339–1349, 2013.

- [17] P. Ranchod, B. Rosman, and G. Konidaris. Nonparametric Bayesian reward segmentation for skill discovery using inverse reinforcement learning. In *IEEE/RSJ International Conference on Intelligent Robots and Systems*, pages 471–477, 2015.
- [18] C. E. Rasmussen and C. K. I. Williams. *Gaussian Processes for machine learning*. MIT Press, 2005.
- [19] A. Šošić, A. M. Zoubir, and H. Koepl. A Bayesian approach to policy recognition and state representation learning. *IEEE Transactions on Pattern Analysis and Machine Intelligence*, 40(6):1295–1308, 2017.
- [20] A. Šošić, E. Rueckert, J. Peters, A. M. Zoubir, and H. Koepl. Inverse reinforcement learning via nonparametric spatio-temporal subgoal modeling. *Journal of Machine Learning Research*, 19(69):1–45, 2018.
- [21] R. S. Sutton and A. G. Barto. *Reinforcement learning: An introduction*. MIT Press, 2018.
- [22] M. K. Titsias. The infinite gamma-Poisson feature model. In *Advances in Neural Information Processing Systems*, pages 1513–1520, 2008.
- [23] F. Wenzel, T. Galy-Fajou, C. Donner, M. Kloft, and M. Opper. Efficient Gaussian process classification using Pölya-gamma data augmentation. *arXiv preprint arXiv:1802.06383*, 2018.

Correlation Priors for Reinforcement Learning

— Supplementary Material —

Bastian Alt^{*}, Adrian Šošić^{*} and Heinz Koepl

Department of Electrical Engineering and Information Technology
Technische Universität Darmstadt

{bastian.alt, adrian.sosic, heinz.koepl}@bcs.tu-darmstadt.de

A Optimizing the Evidence Lower Bound (ELBO)

In this section we derive the calculation for optimizing the ELBO for the presented model. In Appendix A.1 we derive the optimal variational distributions and their parameters. In Appendix A.2 we derive the ELBO as function of the variational parameters.

The ELBO of the presented model is

$$L(q) = \mathbb{E} [\log p(\Psi, \Omega, \mathbf{X})] - \mathbb{E} [\log q(\Psi, \Omega)]. \quad (5)$$

The joint distribution for the model with the PG augmentation scheme is given by

$$\begin{aligned} p(\Psi, \Omega, \mathbf{X}) &= \prod_{k=1}^{K-1} \mathcal{N}(\psi_{\cdot k} \mid \mu_k, \Sigma) \\ &\times \prod_{c=1}^C \binom{b_{ck}}{x_{ck}} 2^{-b_{ck}} \exp(\kappa_{ck} \psi_{ck}) \exp(-\omega_{ck} \psi_{ck}^2 / 2) \text{PG}(\omega_{ck} \mid b_{ck}, 0). \end{aligned} \quad (6)$$

For the derivation we assume a factorized approximation, with

$$q(\Psi, \Omega) = \prod_{k=1}^{K-1} q(\psi_{\cdot k}) \prod_{c=1}^C q(\omega_{ck}). \quad (7)$$

A.1 Calculation of the parametric form of the variational distributions

A.1.1 Calculating the variational distribution $q(\psi_{\cdot k})$

First, we compute the optimal distribution of the variational distributions $q(\psi_{\cdot k})$, $k = 1, \dots, K - 1$. Collecting all terms in Eq. (5) which have a dependence on $\psi_{\cdot k}$ gives

$$L(q) = L(q(\psi_{\cdot k})) + L_{\text{const}}.$$

Due to the factorization in Eq. (7) together with Eq. (6), we have

$$L(q(\psi_{\cdot k})) = \mathbb{E} [\log \mathcal{N}(\psi_{\cdot k} \mid \mu_k, \Sigma)] + \sum_{c=1}^C \mathbb{E} [\psi_{ck}] \kappa_{ck} - \sum_{c=1}^C \mathbb{E} [\omega_{ck} \psi_{ck}^2 / 2] - \mathbb{E} [\log q(\psi_{\cdot k})].$$

The optimal distribution can be calculated by introducing the Lagrangian

$$\begin{aligned} \mathcal{L}(q(\psi_{\cdot k}), \nu) &= \mathbb{E} [\log \mathcal{N}(\psi_{\cdot k} \mid \mu_k, \Sigma)] + \sum_{c=1}^C \mathbb{E} [\psi_{ck}] \kappa_{ck} - \sum_{c=1}^C \mathbb{E} [\omega_{ck} \psi_{ck}^2 / 2] \\ &\quad - \mathbb{E} [\log q(\psi_{\cdot k})] + \nu \left(\int q(\psi_{\cdot k}) d\psi_{\cdot k} - 1 \right), \end{aligned}$$

which ensures that $q(\psi_{\cdot k})$ is a proper density, using ν as a Lagrange multiplier to enforce the normalization constraint. The Euler Lagrange equation and optimality condition are

$$\frac{\delta \mathcal{L}}{\delta q} = 0, \quad \frac{\partial \mathcal{L}}{\partial \nu} = 0. \quad (8)$$

The functional derivative of the Lagrangian yields

$$\frac{\delta \mathcal{L}}{\delta q} = \log \mathcal{N}(\psi_{\cdot k} \mid \boldsymbol{\mu}_k, \boldsymbol{\Sigma}) + \sum_{c=1}^C \psi_{ck} \kappa_{ck} - \sum_{c=1}^C \mathbb{E}[\omega_{ck}] \psi_{ck}^2 / 2 - \log q(\psi_{\cdot k}) - 1 + \nu.$$

By solving the Euler Lagrange equation for $q(\psi_{\cdot k})$, we obtain

$$q(\psi_{\cdot k}) = \exp \left(\nu - 1 + \log \mathcal{N}(\psi_{\cdot k} \mid \boldsymbol{\mu}_k, \boldsymbol{\Sigma}) + \sum_{c=1}^C \psi_{ck} \kappa_{ck} - \sum_{c=1}^C \mathbb{E}[\omega_{ck}] \psi_{ck}^2 / 2 \right).$$

The optimality condition (normalization constraint) in Eq. (8) yields

$$\begin{aligned} q(\psi_{\cdot k}) &\propto \mathcal{N}(\psi_{\cdot k} \mid \boldsymbol{\mu}_k, \boldsymbol{\Sigma}) \exp \left(-\frac{1}{2} \sum_{c=1}^C \mathbb{E}[\omega_{ck}] \psi_{ck}^2 + \sum_{c=1}^C \psi_{ck} \kappa_{ck} \right) \\ &\propto \mathcal{N}(\psi_{\cdot k} \mid \boldsymbol{\mu}_k, \boldsymbol{\Sigma}) \prod_{c=1}^C \mathcal{N}\left(\frac{\kappa_{ck}}{\mathbb{E}[\omega_{ck}]} \mid \psi_{ck}, 1/\mathbb{E}[\omega_{ck}]\right) \\ &= \mathcal{N}(\psi_{\cdot k} \mid \boldsymbol{\mu}_k, \boldsymbol{\Sigma}) \mathcal{N}(\text{diag}(\mathbb{E}[\boldsymbol{\omega}_k])^{-1} \boldsymbol{\kappa}_k \mid \psi_{\cdot k}, \text{diag}(\mathbb{E}[\boldsymbol{\omega}_k])^{-1}). \end{aligned}$$

Therefore, the optimal distribution $q(\psi_{\cdot k})$ can be identified as a Gaussian by completing the square

$$q(\psi_{\cdot k}) = \mathcal{N}(\psi_{\cdot k} \mid \boldsymbol{\lambda}_k, \mathbf{V}_k), \quad (9)$$

with the variational parameters

$$\mathbf{V}_k = (\boldsymbol{\Sigma}^{-1} + \text{diag}(\mathbb{E}[\boldsymbol{\omega}_k]))^{-1}, \quad \boldsymbol{\lambda}_k = \mathbf{V}_k(\boldsymbol{\kappa}_k + \boldsymbol{\Sigma}^{-1} \boldsymbol{\mu}_k). \quad (10)$$

A.1.2 Calculating the variational distribution $q(\omega_{ck})$

In a similar fashion the distribution for $q(\omega_{ck})$ is calculated. The ELBO in Eq. (5) in terms dependent on ω_{ck} can be written as

$$L(q(\omega_{ck})) = L(q(\omega_{ck})) + L_{\text{const}},$$

with

$$L(q(\omega_{ck})) = -\mathbb{E}[\omega_{ck}] \mathbb{E}[\psi_{ck}^2] / 2 + \mathbb{E}[\log \text{PG}(\omega_{ck} \mid b_{ck}, 0)] - \mathbb{E}[\log q(\omega_{ck})].$$

The Lagrangian for the distribution $q(\omega_{ck})$ is

$$\begin{aligned} \mathcal{L}(q(\omega_{ck}), \nu) &= -\mathbb{E}[\omega_{ck}] \mathbb{E}[\psi_{ck}^2] / 2 + \mathbb{E}[\log \text{PG}(\omega_{ck} \mid b_{ck}, 0)] - \mathbb{E}[\log q(\omega_{ck})] \\ &\quad + \nu \left(\int q(\omega_{ck}) d\omega_{ck} - 1 \right) \end{aligned}$$

The functional derivative of the Lagrangian yields

$$\frac{\delta \mathcal{L}}{\delta q} = -\omega_{ck} \mathbb{E}[\psi_{ck}^2] / 2 + \log \text{PG}(\omega_{ck} \mid b_{ck}, 0) - \log q(\omega_{ck}) - 1 + \nu.$$

Solving the Euler Lagrange equation $\frac{\delta \mathcal{L}}{\delta q} = 0$ for $q(\omega_{ck})$, we find

$$q(\omega_{ck}) = \exp \left(\nu - 1 + \log \text{PG}(\omega_{ck} \mid b_{ck}, 0) - \omega_{ck} \mathbb{E}[\psi_{ck}^2] / 2 \right).$$

The normalization constraint is used to identify

$$q(\omega_{ck}) \propto \text{PG}(\omega_{ck} \mid b_{ck}, 0) \exp \left(-\omega_{ck} \mathbb{E}[\psi_{ck}^2] / 2 \right).$$

By exploiting the exponential tilting property of the PG distribution $\text{PG}(\zeta \mid u, v) \propto \exp(-\frac{v^2}{2}\zeta) \text{PG}(\zeta \mid u, 0)$ we obtain

$$q(\omega_{ck}) = \text{PG}(\omega_{ck} \mid b_{ck}, w_{ck}), \quad (11)$$

with the variational parameter $w_{ck} = \sqrt{\mathbb{E}[\psi_{ck}^2]}$.

A.2 The ELBO for the optimal distributions

The ELBO

$$L(q) = \mathbb{E} [\log p(\Psi, \Omega, \mathbf{X})] - \mathbb{E} [\log q(\Psi, \Omega)]$$

in terms of the previously derived optimal distributions calculates to

$$\begin{aligned} \mathbb{E} [\log p(\Psi, \Omega, \mathbf{X})] &= \sum_{k=1}^{K-1} \mathbb{E} [\log \mathcal{N}(\psi_{\cdot k} | \mu_k, \Sigma)] + \sum_{k=1}^{K-1} \sum_{c=1}^C \log \left(\frac{b_{ck}}{x_{ck}} \right) \\ &\quad - \sum_{k=1}^{K-1} \sum_{c=1}^C b_{ck} \log 2 + \sum_{k=1}^{K-1} \lambda_k^\top \kappa_k \\ &\quad + \sum_{k=1}^{K-1} \sum_{c=1}^C \mathbb{E} [\log \text{PG}(\omega_{ck} | b_{ck}, w_{ck})] \\ &\quad - \sum_{k=1}^{K-1} \sum_{c=1}^C b_{ck} \log \left(\cosh \frac{w_{ck}}{2} \right), \\ \mathbb{E} [\log q(\Psi, \Omega)] &= \sum_{k=1}^{K-1} \mathbb{E} [\log \mathcal{N}(\psi_{\cdot k} | \lambda_k, \mathbf{V}_k)] + \sum_{k=1}^{K-1} \sum_{c=1}^C \mathbb{E} [\log \text{PG}(\omega_{ck} | b_{ck}, w_{ck})]. \end{aligned}$$

The terms $\mathbb{E} [\log \text{PG}(\omega_{ck} | b_{ck}, w_{ck})]$ cancel out and collecting prior and variational terms as Kullback-Leibler (KL) divergence we obtain

$$\begin{aligned} L(q) &= - \sum_{k=1}^{K-1} \text{KL}(\mathcal{N}(\psi_{\cdot k} | \lambda_k, \mathbf{V}_k) \parallel \mathcal{N}(\psi_{\cdot k} | \mu_k, \Sigma)) + \sum_{k=1}^{K-1} \sum_{c=1}^C \log \left(\frac{b_{ck}}{x_{ck}} \right) \\ &\quad - \sum_{k=1}^{K-1} \sum_{c=1}^C b_{ck} \log 2 + \sum_{k=1}^{K-1} \lambda_k^\top \kappa_k - \sum_{k=1}^{K-1} \sum_{c=1}^C b_{ck} \log \left(\cosh \frac{w_{ck}}{2} \right). \end{aligned}$$

Finally, by computing the KL divergence, the ELBO dependent on the variational parameters is

$$\begin{aligned} L(q) &= - \frac{K-1}{2} |\Sigma| + \frac{1}{2} \sum_{k=1}^{K-1} \log |\mathbf{V}_k| - \frac{1}{2} \sum_{k=1}^{K-1} \text{tr}(\Sigma^{-1} \mathbf{V}_k) \\ &\quad - \frac{1}{2} \sum_{k=1}^{K-1} (\mu_k - \lambda_k)^\top \Sigma^{-1} (\mu_k - \lambda_k) + C(K-1) + \sum_{k=1}^{K-1} \sum_{c=1}^C \log \left(\frac{b_{ck}}{x_{ck}} \right) \\ &\quad - \sum_{k=1}^{K-1} \sum_{c=1}^C b_{ck} \log 2 + \sum_{k=1}^{K-1} \lambda_k^\top \kappa_k - \sum_{k=1}^{K-1} \sum_{c=1}^C b_{ck} \log \left(\cosh \frac{w_{ck}}{2} \right). \end{aligned} \quad (12)$$

B Derivation for hyper parameter optimization

In this section we give a derivation for the optimization of the hyper parameters. By maximizing the ELBO $L(q)$ w.r.t. to the parameters μ_k and the parameterized covariance matrix Σ_θ we obtain equations for the variational expectation maximization algorithm.

The ELBO as a function of the mean μ_k and covariance Σ_θ can be written as

$$\begin{aligned} L(\Sigma_\theta, \mu_k) &= - \frac{K-1}{2} |\Sigma_\theta| - \frac{1}{2} \sum_{k=1}^{K-1} \text{tr}(\Sigma_\theta^{-1} \mathbf{V}_k) \\ &\quad - \frac{1}{2} \sum_{k=1}^{K-1} (\mu_k - \lambda_k)^\top \Sigma_\theta^{-1} (\mu_k - \lambda_k) + L_{const}. \end{aligned} \quad (13)$$

B.1 Derivation for the optimal value for the mean μ_k

We calculate the gradient of Eq. (13) as

$$\frac{\partial L}{\partial \mu_k} = \Sigma_{\theta}^{-1} (\mu_k - \lambda_k).$$

Setting the gradient to zeros we obtain

$$\mu_k = \lambda_k. \quad (14)$$

B.2 Derivation for the optimal hyper parameters of Σ_{θ}

We calculate the gradient of Eq. (13) as

$$\begin{aligned} \frac{\partial L}{\partial \theta_j} = & -\frac{K-1}{2} \text{tr}(\Sigma_{\theta}^{-1} \frac{\partial \Sigma_{\theta}}{\partial \theta_j}) + \frac{1}{2} \sum_{k=1}^{K-1} \text{tr}(\Sigma_{\theta}^{-1} \frac{\partial \Sigma_{\theta}}{\partial \theta_j} \Sigma_{\theta}^{-1} \mathbf{V}_k) \\ & + \frac{1}{2} \sum_{k=1}^{K-1} (\mu_k - \lambda_k)^{\top} \Sigma_{\theta}^{-1} \frac{\partial \Sigma_{\theta}}{\partial \theta_j} \Sigma_{\theta}^{-1} (\mu_k - \lambda_k). \end{aligned} \quad (15)$$

When assuming the special case of a scaled covariance matrix $\Sigma_{\theta} = \theta \tilde{\Sigma}$, we can find the optimizing hyper parameter θ in closed form. Note that $\frac{\partial \Sigma_{\theta}}{\partial \theta} = \tilde{\Sigma}$ and $\Sigma_{\theta}^{-1} = \frac{1}{\theta} \tilde{\Sigma}^{-1}$.

Therefore, the gradient computes to

$$\frac{\partial L}{\partial \theta} = -\frac{K}{2\theta} \text{tr}(\mathbf{I}) + \frac{1}{2\theta^2} \sum_{k=1}^{K-1} \text{tr}(\tilde{\Sigma}^{-1} \mathbf{V}_k) + \frac{1}{2\theta^2} \sum_{k=1}^{K-1} (\mu_k - \lambda_k)^{\top} \tilde{\Sigma}^{-1} (\mu_k - \lambda_k).$$

Setting the derivative to zero and solving for θ , we obtain the closed form expression

$$\theta = \frac{1}{KS} \sum_{k=1}^{K-1} \text{tr} \left(\tilde{\Sigma}^{-1} (\mathbf{V}_k + (\mu_k - \lambda_k)(\mu_k - \lambda_k)^{\top}) \right). \quad (16)$$